J. Fluid Mech. (1992), *vol.* 235, *pp.* 73–87
Printed in Great Britain

Spherical cap bubbles

By YUMIN YANG† AND HERBERT LEVINE

Department of Physics *and* Institute for Nonlinear Science, University of California, San Diego, La Jolla, CA 92093-0075, USA

(Received 7 March 1990 and in revised form 20 June 1991)

We study the rise of a spherical cap bubble in both two- and three-dimensional unbounded regions. In particular we focus on the problem of finding steady state-solutions. We assume that the fluid is incompressible, inviscid and irrotational, and use two different models to approximate the turbulent wake behind the bubble. We demonstrate numerically that in the case of zero surface tension we have a continuous spectrum of rise velocities. When we add small surface tension to the problem, the degeneracy is broken via a solvability mechanism, and we obtain velocity selection. Our results are in good agreement with the existing experimental studies.

1. Introduction

The problem of a spherical cap bubble rising in an unbounded region of a fluid in two or three dimensions has been studied both theoretically and experimentally over the past few decades, see Collins (1965), Grace & Harrison (1967), Maneri & Zuber (1974), Davies & Taylor (1950), Hnat & Buckmaster (1976) and Collins (1967*a*). (For additional references, see the review paper by Wegener & Parlange 1973.) Experimentally one always finds that the bubble rises at a constant speed after an initial acceleration. To date, there is no first-principles theory which determines this rise velocity for all the relevant experimental cases (especially for three-dimensional bubbles).

Early theoretical treatments often ignored suface tension, which is indeed very small. However, it will be shown in this paper that the small surface tension perturbation is a singular one and it plays a crucial role in determining the rise velocity of the bubble. This point was first made by Vanden-Broeck (1986, 1988) in terms of two-dimensional spherical cap bubbles. We shall compare our numerical results with his later in this paper.

In recent years, several authors, Vanden-Broeck (1984*a*, *b*), Couët & Strumolo (1987), Kessler & Levine (1989*a*) and Levine & Yang (1990), have worked on the problem of an infinitely long bubble rising in a channel (two-dimensional) or a tube (three-dimensional). There it was found through numerical work that the bubble rising velocity is indeed determined by the surface tension, and the small-surface-tension limit is a singular perturbation of the zero-surface-tension situation (i.e. taking the limit of surface tension approaching zero is *not* the same as setting it to zero). The conclusions of the spherical cap bubble theory here resemble those of the infinitely long bubble in many ways.

We now describe the notation we will use throughout this paper. The coordinate

† Present address: Department of Applied Mathematics and Statistics, SUNY at Stony Brook, Stony Brook, NY 11794–3600, USA.

axes x and y denote the horizontal and vertical directions respectively. Gravity is in the $-\hat{y}$ direction. For the two-dimensional bubble, x and y are Cartesian coordinates. For the three-dimensional bubble, x and y should be regarded as cylindrical coordinates, i.e. $x \to r, y \to z$. We choose our units such that $R_w = g = \rho = 1$, where R_w is the half-width of the bottom of the spherical cap bubble, g is the gravitational acceleration, and ρ is the density of the fluid. In these units, the dimensionless rise velocity u is just the Froude number of the flow, i.e. $u \equiv Fr_w = u^*/(gR_w)^{\frac{1}{2}}$, where u^* is the physical rise velocity; also, the dimensionless surface tension coefficient γ is the inverse Eötovos number, i.e. $\gamma = \gamma^*/(\rho g R_w^2)$, where γ^* is the dimensional surface tension coefficient. Note that there are two other lengths in this problem; R_c, which is the radius of curvature at the tip, and R_v, which is the equivalent of volume. The experimental Froude numbers are often expressed in terms of these two lengths, i.e. $Fr_c = u^*/(gR_c)^{\frac{1}{2}}$ and $Fr_v = u^*/(gR_v)^{\frac{1}{2}}$. We choose R_w to be the unit length simply for computational convenience. Once the bubble profile is known, we can easily convert Fr_w into Fr_c and Fr_v, which can then be compared with experiments.

2. Formulation

Before describing our formulation of the bubble problem, we would like to note a difference between the two-dimensional and three-dimensional cases. In the two-dimensional bubble problem, both the stream function and potential function satisfy the Laplace equation, and form the imaginary and real parts of an analytic function. Thus the powerful tools of complex analysis can be used in this situation. Most of papers mentioned in the introduction, e.g. Vanden-Broeck (1984*a*, *b*, 1986, 1988) and Couët & Strumolo (1987), use this technique to attack two-dimensional bubble problems. For the three-dimensional problem, this technique no longer applies because the stream function does not satisfy the Laplace equation (see (15)). Our formulation below in terms of Green's function closely resembles those by Kessler & Levine (1989*a*) and Levine & Yang (1990) for the bubble in a tube. One of the advantages of this approach is that the two- and three-dimensional cases can be treated in parallel.

Let us first outline the assumptions that we will make for this problem. The first is that the fluid is inviscid. This is due to the experimental fact that the rise velocity (Froude number) of a spherical cap bubble is independent of the Reynolds number when the Reynolds number is large enough (~ 100), see Hnat & Buckmaster (1976) and Wegener & Parlange (1973). We next assume that the fluid is of constant density and irrotational outside the wake and bubble interior. The first part of this assumption is valid because the bubble rise velocity is much smaller than the speed of sound; the secnd part is also very reasonable since the fluid is stationary before the bubble passes through. We also neglect the density of the gas inside the bubble. Since we are only considering the case of a spherical cap bubble rising in an unbounded region, the bubble will rise along a vertical path. Hence we can further assume that the flow is symmetric (two-dimensional) or axisymmetric (three-dimensional). The assumption of axisymmetry for the three-dimensional spherical cap bubble problem allows us to reduce the three-dimensional problem into an effective two-dimensional one.

Because the bubble rises at a constant speed, one can transform to a moving frame and look for steady-state solutions. However, it is clear from experiments that there is a turbulent wake behind a rising spherical cap bubble at high Reynolds number, see Van Dyke (1982) and Maxworthy (1967), and the entire flow is not stationary

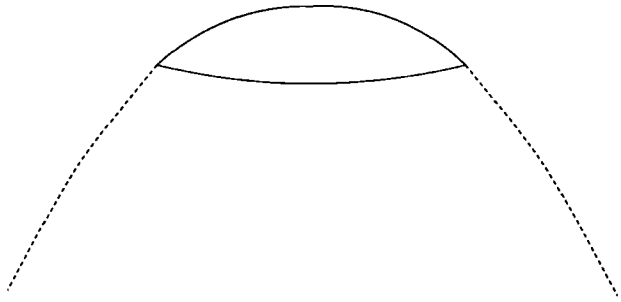

FIGURE 1. Sketch of the bubble shape and wake boundary for the stagnant wake model.

even in the moving frame. In this paper, we shall nonetheless assume that the flow is stationary outside the wake and bubble interior. Instead of dealing with a realistic turbulent wake, we approximate the wake by two different models, which makes sense because we expect the bubble rise velocity to be determined by the bubble tip region and hence should be insensitive to the exact form of the wake. The experimental evidence supporting this idea comes from the work of Grace & Harrison (1967). They placed a vertical rod in the path of a spherical cap bubble, and found that the rod affected the bubble most when located exactly at the centre. Theoretically, the action of the surface tension as a singular perturbation will be most crucial near the tip, as seen from the approximate model by Kessler & Levine (1989*a*). The two models that we shall use are the stagnant wake model and the vertical wake model, which we now describe.

The first model approximates the dynamic wake by a stagnant one (Vanden-Broeck 1986; Rippin & Davidson 1967), see figure 1. The balance of hydrostatic pressure inside the wake and the pressure outside tells us that the speed of the flow on the wake boundary is a constant, i.e. the wake boundary is a vortex sheet. Furthermore one can easily prove that this constant speed is the same as the flow speed at infinity (we are in the moving frame), which is the bubble rising velocity u. In this model, the shape of the wake boundary is not known *a priori*, but the velocity distribution on the boundary is known. The wake shape has to be solved consistently with the bubble shape in the whole problem. However, the asymptotic shape ($y \to -\infty$) of the stagnant wake is known (Gurevich 1965); in two dimensions it is

$$x = a(-y)^{\frac{1}{2}}, \tag{1}$$

and in three-dimensions it is (also see Levinson 1946)

$$x = a(-y)^{\frac{1}{2}}/[\ln(-y)]^{\frac{1}{4}}, \tag{2}$$

where the coefficient a depends on the bubble shape.

The second model approximates the wake shape by a vertical line extending to minus infinity (Vanden-Broeck 1988), see figure 2. There are several reasons to propose this model. First, the pictures taken by Maxworthy (1967) show us that the shape of the real bubble wake does look somewhat like this; secondly, there is one known analytic solution to this model, namely the Zhukovskii solution, see Vanden-Broeck (1988), Gurevich (1965) and Collins (1967*b*). This solution tells us that when a two-dimensional spherical cap bubble with no surface tension rises at a velocity of $1/\pi^{\frac{1}{2}}$, the bubble shape will be

$$x = \frac{2}{\pi}(\theta + \tfrac{1}{2}\sin 2\theta), \qquad y = -\frac{2}{\pi}\sin^2\theta, \tag{3a, b}$$

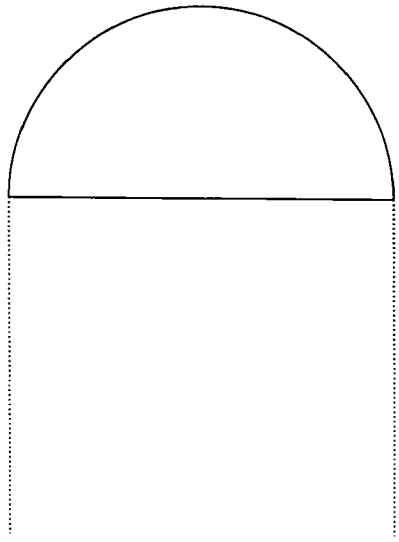

FIGURE 2. Sketch of the bubble shape and wake boundary for the vertical wake model.

where the parameter θ goes from 0 to $\frac{1}{2}\pi$. Now, if one assumes that the fluid inside the wake is stagnant, then one immediately discovers that the pressure across the wake boundary is not continuous. For this reason, this model has historically been regarded as being completely unrealistic. We would like to suggest that since the wake is turbulent, fluctuations might be able to balance the pressure outside. Thus this model could be realistic, and in fact it will be shown later that it approximates the experimental data better than the stagnant wake model. In this model, the shape of the wake boundary is known *a priori*, but the velocity distribution on the boundary is not known. The velocity distribution has to be solved consistently with the bubble shape in the whole problem. Nevertheless, one can easily show that the asymptotic velocity ($y \to -\infty$) on the wake boundary is just the bubble rise velocity u for both the two- and three-dimensional cases.

For both models, the wake is required to attach to the top of the bubble smoothly, in the sense that the first derivative is continuous.

With the above qualitative pictures in mind, we now formulate the spherical cap bubble problem quantitatively. We will do this first for the two-, then the three-dimensional bubble: the two formulations are analogous. We write both of them down here for completeness.

2.1. *The two-dimensional case*

Since the velocity field is divergence free, we can define the stream function as follows:

$$\boldsymbol{v} = \nabla \times [\psi(x, y)\, \hat{\boldsymbol{z}}]. \tag{4}$$

The irrotational condition gives us the following equation for ψ:

$$\frac{\partial^2 \psi}{\partial x^2} + \frac{\partial^2 \psi}{\partial y^2} = 0. \tag{5}$$

Having derived the equation for ψ, let us determine the boundary conditions that ψ should satisfy. Since the flow at infinity is uniformly slowing down, we have

$$\psi|_{\infty} = -ux. \tag{6}$$

On the bubble surface and the wake boundary, the stream function ψ is a constant. We can let this constant be zero without loss of generality, i.e.

$$\psi|_{y=\eta(x)} = 0, \tag{7}$$

$$\psi|_{y=\zeta(x)} = 0, \tag{8}$$

where we denoted the bubble surface by $y = \eta(x)$, and the wake boundary by $y = \zeta(x)$. Bernoulli's law on the bubble surface for the stationary flow provides us with another boundary condition,

$$\frac{1}{2}\left|\frac{\partial\psi(x,y)}{\partial n}\right|^2|_{y=\eta(x)} + \eta(x) - \gamma\kappa(x) = 0. \tag{9}$$

Here κ is the mean curvature of the surface, which can be written as

$$\kappa(x) = -\frac{\eta''}{(1+\eta'^2)^{\frac{3}{2}}}, \tag{10}$$

where η' and η'' denote $\mathrm{d}\eta/\mathrm{d}x$ and $\mathrm{d}^2\eta/\mathrm{d}x^2$ respectively.

Had the bubble surface been given, we would have overspecified the boundary conditions. Since this is a free boundary problem, we can use the extra boundary condition (9) to determine the bubble shape. We will use Green's function method to obtain integro-differential equations for the bubble shape $\eta(r)$. The Green's function in this case is

$$G(x,x',y,y') = -\frac{1}{4\pi}\ln\frac{(x-x')^2+(y-y')^2}{(x+x')^2+(y-y')^2}, \tag{11}$$

which is just the antisymmetrized (around the y-axis) free Green's function for the two-dimensional Laplace equation.

In terms of this Green's function, ψ can be written as

$$\psi(x,y) = -ux + \int_0^\infty G(x,x',y,y')\frac{\partial\psi}{\partial n'}\mathrm{d}s'. \tag{12}$$

Since our Green's function is antisymmetric, we only have to integrate over half of the free surface. Setting $y = \eta(x)$, $y = \zeta(x)$ and substituting (9) into (12), we obtain the set of integro-differential equations we want:

$$-ux + \int_0^{s_0'} G(x,x',\eta(x),\eta(x'))\,[2\gamma\kappa(x') - 2\eta(x')]^{\frac{1}{2}}\,\mathrm{d}s' + \int_{s_0'}^\infty G(x,x',\eta(x),\zeta(x'))\,v_{\mathrm{wk}}\,\mathrm{d}s' = 0, \tag{13a}$$

$$-ux + \int_0^{s_0'} G(x,x',\zeta(x),\eta(x'))\,[2\gamma\kappa(x') - 2\eta(x')]^{\frac{1}{2}}\,\mathrm{d}s' + \int_{s_0'}^\infty G(x,x',\zeta(x),\zeta(x'))\,v_{\mathrm{wk}}\,\mathrm{d}s' = 0. \tag{13b}$$

At the arclength s_0', the bubble surface meets the wake. It is quite clear that these two equations are coupled. The first is valid for a point on the bubble surface, the second for a point on the wake boundary. The difference between the stagnant and the vertical wake models in (13) is that, for the former, ζ is unknown but v_{wk} is known; for the latter, the situation is reversed.

2.2. *The three-dimensional case*

Since the velocity field is divergence free and axisymmetric, the Stokes' stream function (see Lamb (1932) can be defined as follows:

$$\boldsymbol{v} = \nabla \times \left[\frac{\psi(x,y)}{x}\hat{\boldsymbol{\phi}}\right], \tag{14}$$

where $\hat{\boldsymbol{\phi}}$ is the unit vector in the angle direction of a cylindrical coordinate system.

The irrotational condition gives us the following equation for ψ:

$$\frac{\partial^2\psi}{\partial x^2} - \frac{1}{x}\frac{\partial\psi}{\partial x} + \frac{\partial^2\psi}{\partial y^2} = 0. \tag{15}$$

Having derived the equation for ψ, let us determine the boundary conditions that ψ should satisfy. Since the flow at infinity is uniformly slowing down, we have

$$\psi|_\infty = -\tfrac{1}{2}ux^2. \tag{16}$$

On the bubble surface and the wake boundary, we have

$$\psi|_{y=\eta(x)} = 0, \tag{17}$$

$$\psi|_{y=\zeta(x)} = 0. \tag{18}$$

Bernoulli's law on the bubble surface for the stationary flow provides us with another boundary condition,

$$\frac{1}{2}\frac{1}{x^2}\left|\frac{\partial\psi(x,y)}{\partial n}\right|^2|_{y=\eta(x)} + \eta(x) - \gamma\kappa(x) = 0. \tag{19}$$

Here κ is the mean curvature of the three-dimensional spherical-cap shaped surface, which can be written as

$$\kappa(x) = -\frac{\eta'}{x(1+\eta'^2)^{\frac{1}{2}}} - \frac{\eta''}{(1+\eta'^2)^{\frac{3}{2}}}. \tag{20}$$

We use Green's function method to derive a pair of integro-differential equations for the bubble shape $\eta(x)$. The free Green's function for (15) in this case is

$$G(x,x',y,y') = \frac{1}{2\pi}(xx')^{\frac{1}{2}}Q_{\frac{1}{2}}\left[1 + \frac{(x-x')^2+(y-y')^2}{2xx'}\right], \tag{21}$$

where $Q_{\frac{1}{2}}$ is the Legendre function of the second kind of order $\frac{1}{2}$.

The derivation is the same as the two-dimensional case and results in the final set of integral-differential equations,

$$-\tfrac{1}{2}ux^2 + \int_0^{s_0'} G(x,x',\eta(x),\eta(x'))\,[2\gamma\kappa(x') - 2\eta(x')]^{\frac{1}{2}}\,\mathrm{d}s' + \int_{s_0'}^{\infty} G(x,x',\eta(x),\zeta(x'))\,v_{\mathrm{wk}}\,\mathrm{d}s' = 0, \tag{22a}$$

$$-\tfrac{1}{2}ux^2 + \int_0^{s_0'} G(x,x',\zeta(x),\eta(x'))\,[2\gamma\kappa(x') - 2\eta(x')]^{\frac{1}{2}}\,\mathrm{d}s' + \int_{s_0'}^{\infty} G(x,x',\zeta(x),\zeta(x'))\,v_{\mathrm{wk}}\,\mathrm{d}s' = 0. \tag{22b}$$

So far we have derived the set of integro-differential equations for both the two-

and three-dimensional spherical cap bubble problem. For a physically meaningful solution of the integro-differential equations (13) and (22) for each case, we must require

$$\eta'|_{x=0} = 0. \tag{23}$$

We will proceed to solve numerically the integro-differential equations (13) and (22) with the boundary condition (23).

3. Numerical procedures

The two- and three-dimensional integro-differential equations (13) and (22) are solved by exactly the same numerical method. We first make an initial guess for the bubble shape and the wake shape or velocity which has the correct asymptotic behaviour far down the wake. We then modify the bubble shape by adding $\Delta\eta$ to the initial guess, and also modify the wake boundary or wake velocity (depending on which model one is using) by adding $\Delta\zeta$ or Δv_{wk} to their initial guesses. We discretize the interface with a fixed grid which becomes an equal-arclength grid downstream. This procedure replaces the integro-differential equation with a coupled set of nonlinear equations, see Kessler & Levine (1989*a*, *b*).

The wake will always be divided into two parts. The lower part is fixed by using the corresponding asymptotic behaviour. For the two-dimensional problem, the wake height is chosen to be around 15; for the three-dimensional problem, it is around 10. The reason for using a shorter wave height in the latter case is that the Green's function decays faster with respect to y (two-dimensional: y^{-2}; three: y^{-3}). It turns out that the bubble tip properties are completely insensitive to the choice of the wake height. All the integrations in our programs are done using Simpson's rule, and the derivatives are evaluated by the three-point rule.

For the zero surface tension case, the independent variables are $N_{bs}\,\Delta\eta$ on the bubble surface, and $N_{wk}\,\Delta\zeta$ or $N_{wk}\,\Delta v_{wk}$ on the wake boundary. The set of integro-differential equations (13) or (22) provides the equations to be satisfied (one for each point, N_{bs} on the bubble surface and N_{wk} on the wake boundary). The values of N_{bs} and N_{wk} we used in our calculation are about 50 and 90 respectively. We now have $N_{bs}+N_{wk}$ variables and $N_{bs}+N_{wk}$ equations, and we use the standard Newton's method to solve them. In fact for the stagnant wake model, we have one more variable, which is the coefficient in the form of the asymptotic shape (1) or (2). The requirement of tangential continuity on the wake boundary provides us with the additional equation needed.

In the case of non-zero surface tension, we used the same method for the wake part as described before, but adopted a different numerical treatment for the bubble surface which we now describe. We will leave the variable v_{bs} in the set of integro-differential equations (13) or (22) instead of substituting it using Bernoulli's law (9) and (19). We now can vary not only $\Delta\eta$, but also Δv_{bs}. We next expand both $\Delta\eta$ and Δv_{bs} in term of Chebyshev polynomials. The coefficients of an expansion will typically converge rapidly for a well-behaved function. We choose the $2n$ coefficients of the expansion (n for $\Delta\eta$ and n for Δv) to be the independent variables. We then pick n points uniformly among the N_{bs} discretized points on the bubble surface of the initial guess. The first integro-differential equation in the set (13) or (22) and Bernoulli's law at these n points will provide us with $2n$ equations to be solved by Newton's method. The typical values for n and N_{bs} used in our program are about 14 and 60. The tangential continuity at the connection point is also enforced in this case.

After obtaining the solution, we check whether the integro-differential equation and Bernoulli's law mentioned above are satisfied on the other discretized points. The results are satisfactory ($\sim 10^{-5}$), except for the points around the connection point with the wake ($\sim 10^{-2}$). As γ decreases, the discrepancy around the connection point becomes smaller. The physical reason for this discrepancy is that both models are ill-defined when the surface tension is non-zero. This is due, of course, to our oversimplified wake assumptions. This solution breakdown at the connection point does not affect the tip region much and hence can be neglected. We will return to expand on this point in §5.

The boundary condition (23) is usually relaxed when we solve the set of integro-differential equations. We check the boundary condition afterwards to see whether it is satisfied. If it is not satisfied, we then move around in the parameter space u and γ until it is.

We now make a few remarks with respect to our numerical methods. Our first remark is on the Green's function (11) or (21): it has a logarithmic singularity when $x \to x'$ and $y \to y'$. This singularity has to be subtracted out when performing the integral in (13) or (22). The logarithmic function $\ln|s-s'|$ can be integrated explicitly along the interface. Thus we can add back in the integral contribution from the singular part of the Green's function. We refer readers to the paper by Kessler & Levine (1989*b*) for more detailed information on this. The second remark is on the three-dimensional curvature formula (20). We will replace η' by $\eta' - (1-x)^2 \eta'|_{x=0}$ there. This is because we wish to allow solutions with non-zero slope at the bubble tip to be found. If we do not make this adjustment, the first term in the curvature will blow up. Since we are eventually interested only in those solutions with zero slope, this adjustment does not alter those 'physical' solutions. The final remark concerns error estimates for our numerical methods. It is quite difficult to get a precise upper bound on the error when there are so many 'freedoms' in the problem. In practice we vary the different discretization parameters in the problem, and find that the final answers are always within a few percent (about 5%).

4. Results

4.1. *Zero surface tension*

To study the system at zero surface tension, we pick a rise velocity u and converge to a bubble solution. We find that the slope at the tip is always small (about 10^{-4}) for a wide range of u. This tells us that there is a continuous spectrum. In other words we cannot get a unique rise velocity from these models with zero surface tension.

When we increase u, the volume of the bubble increases (see figures 3 and 4), and the radius of curvature at the bubble tip decreases (see figures 5 and 6). The curve in figure 5 or 6 will level off at a value of u at which the slope at the tip will change rapidly from almost zero to a negative number. The velocity at which this occurs depends on the discretization of the bubble at the tip region. The larger the grid, the smaller this velocity will be. We interpret this phenomenon as due to the finite grid size which limits the tip curvature that we can resolve. As we decrease the grid size at the tip, the velocity at which level-off occurs will approach a limit value u_*, at which the radius of curvature at the tip will be zero. Consequently, the slope at the tip is no longer equal to zero when the rise velocity is larger than u_*. This tells us that the set of integro-differential equation (13) or (22) with the boundary (23) has a continuous spectrum of rise velocity up to a certain velocity u_* in the zero surface tension case. This is true for both the stagnant and the vertical wake modes. In fact

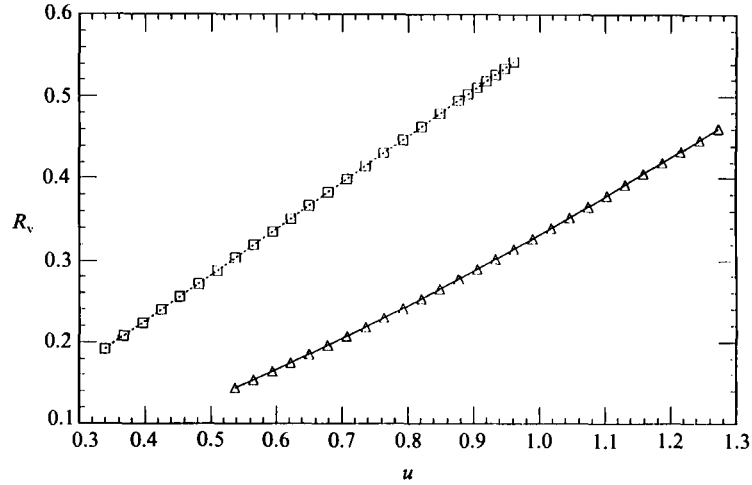

FIGURE 3. Radius of volume *vs.* the rise velocity for the two-dimensional spherical cap bubble with zero surface tension: —△—, stagnant wake; --□--, vertical wake.

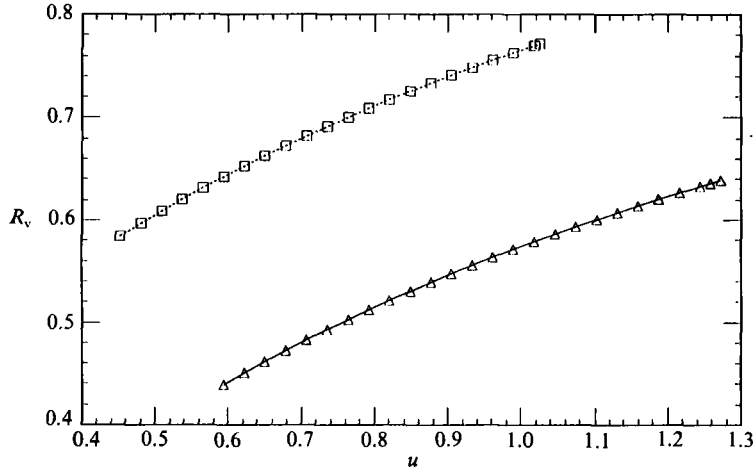

FIGURE 4. Radius of volume *vs.* the rise velocity for the three-dimensional spherical cap bubble with zero surface tension. Notation as figure 3.

it is quite clear from figures 3–6 that the stagnant and vertical wake models have the same qualitative but different quantitative behaviour, as do the two- and three-dimensional bubbles.

For the two-dimensional spherical cap bubble, our calculated u_* of the stagnant wake model is about 1.29, and the u_* of the vertical wake model is about 0.96, which are in agreement with the previous work by Vanden-Broeck (1986, 1988). The corresponding u_* values for the three-dimensional spherical cap bubble problem are 1.27 (stagnant wake) and 1.04 (vertical wake).

From the results above we see that the Zhukovskii analytic solution (3) is only one particular solution among a family of solutions for the two-dimensional vertical wake model.

4.2. *Non-zero surface tension*

In the presence of surface tension, we fix the surface tension coefficient γ, and vary the rise velocity u. We then relax the boundary condition (23) and solve the set of integro-differential equations. We find that within a narrow region of a certain rise

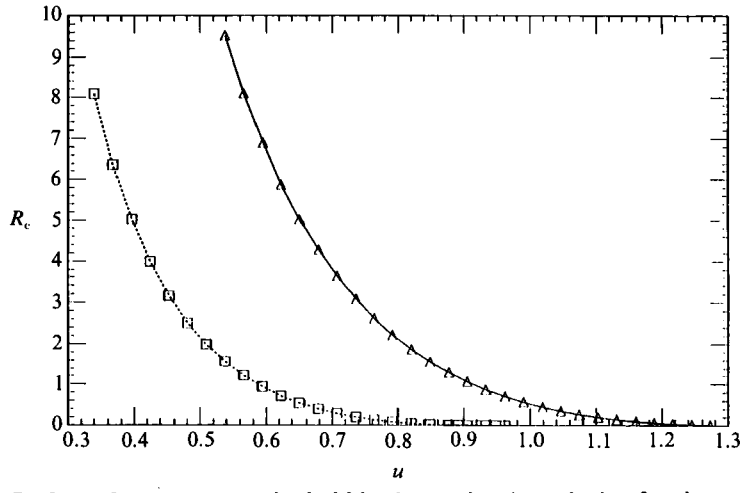

FIGURE 5. Radius of curvature at the bubble tip *vs.* the rise velocity for the two-dimensional spherical cap bubble with zero surface tension. Notation as figure 3.

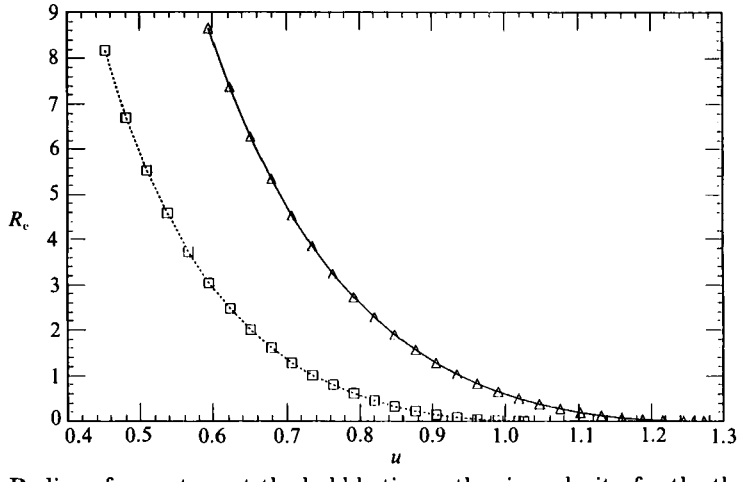

FIGURE 6. Radius of curvature at the bubble tip *vs.* the rise velocity for the three-dimensional spherical cap bubble with zero surface tension. Notation as figure 3.

velocity u_0 ($\Delta u \sim \pm 0.03$), the slope at the bubble tip changes by several orders of magnitude, from about $\sim 10^{-2}$ to about $\sim -10^{-2}$, i.e. it clearly goes through zero. Since the only physical solution is the one with the zero slope at the bubble tip, we see that the degeneracy of the zero surface tension situation is broken, i.e. there is a velocity selection.

Since we are only interested in the limit of surface tension approaching zero, only a small surface tension is added to the problem. In our calculation, we choose γ to be 5×10^{-3}. A physical system corresponding to such a γ could be a spherical cap air bubble of bottom diameter about 3 in. rising in water. The Reynolds number for such a flow is on the order of 10000.

The major results of this study are summarized in table 1, where we compare the rise velocities (selected through the aforementioned mechanism) in our theory with the corresponding experimental ones. θ_0 in the table is the angle between the centre axis and the edge of the bubble measured from the centre of curvature at the tip. The

	Two-dimensional				Three-dimensional			
	Fr_w	Fr_c	Fr_v	θ_0 (deg.)	Fr_w	Fr_c	Fr_v	θ_0 (deg.)
Stagnant	0.84	0.63	1.64	36	0.88	0.69	1.20	40
Vertical	0.57	0.50	1.00	60	0.71	0.64	0.85	61
Experimental		0.55	1.12	53		0.65	1.03	50

TABLE 1. Comparison between the theoretical and experimental results

two blank spaces mean that there are no experimental data available. The experimental results for a two-dimensional spherical cap bubble in the table for Fr_c and θ_0 are from Collins (1965); Fr_v are from Maneri & Zuber (1974), where we used the data presented in their figure 6(*a*) extrapolated to zero spacing between the two vertical plates. The experimental results for a three-dimensional spherical cap bubble for Fr_c are from Collins (1967*a*); Fr_v are from several sources (Davies & Taylor 1950; Wegener & Parlange 1973; Hnat & Buckmaster 1976); θ_0 are from Wegener & Parlange (1973).

From the table we see that the agreement between the theoretical and experimental results for Fr_c is quite good, especially for the three-dimensional bubble. This is because Fr_c only depends on the local properties of the bubble tip, which are lest influenced by the wake. Not surprisingly, the agreement between the theory and experiments for Fr_v and θ_0 is less impressive, since the nature of the wake plays a relatively large role in these two quantities. It is obvious from the table that the vertical wake model approximates the experimental data better than the stagnant wake model. This is probably because the real spherical cap bubble wake shape resembles more closely that in the vertical wake model than that in the stagnant wake model, see pictures in Maxworthy (1967).

For the two-dimensional spherical cap bubble problem, our calculated Fr_w for the stagnant wake model is in agreement with figure 5 of Vanden-Broeck's (1986) paper;† for the vertical wake model, we also agree with Vanden-Broeck (1988) that the selected solution in the zero surface tension limit is precisely the Zhukovskii solution.

We also made a different run using our computer programs with the same parameters except for a factor of two in the surface tension, i.e. $\gamma = 0.01$. We found that the numbers given in table 1 stayed almost the same. This tells us that the selected rise velocity in the small-surface-tension limit is not especially sensitive to the surface tension. It is known that this is true for the problem of an infinitely long bubble rising in a channel (two dimensions) or a tube (three dimensions); in other words, the solution curve in the (u, γ) parameter plane intersects the u-axis with a 90° angle, see Vanden-Broeck (1984*b*), Couët & Strumolo (1987), Kessler & Levine (1989*a*) and Levine & Yang (1990). This helps us to explain the experimental fact that when water is replaced by methanol (surface tension is three times smaller), no difference in the bubble rise velocity is exhibited, see Maneri & Zuber (1974).

The curvature at the tip region is almost a constant for all four selected solutions (both models and dimensions). Thus they resemble spherical caps (at least in the tip

† Vanden-Broeck used two different methods to obtain this Froude number. The results of these two methods did not agree with each other very well. This is probably because there is a hidden singularity in the problem. We will come back to this point in §5.

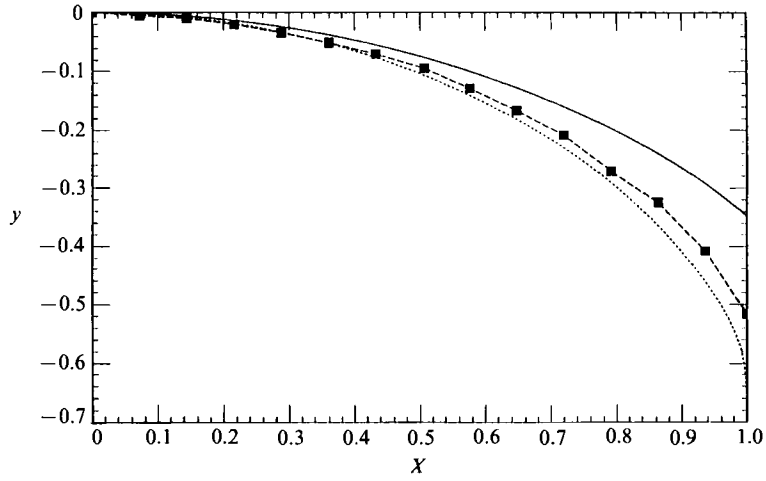

FIGURE 7. Comparison between the calculated bubble profiles, and the corresponding experimental one (figure 4*a* in Grace & Harrison 1967) for the two-dimensional spherical cap bubble: ——, stagnant wake, – – – –, vertical wake; – –■– –, experimental.

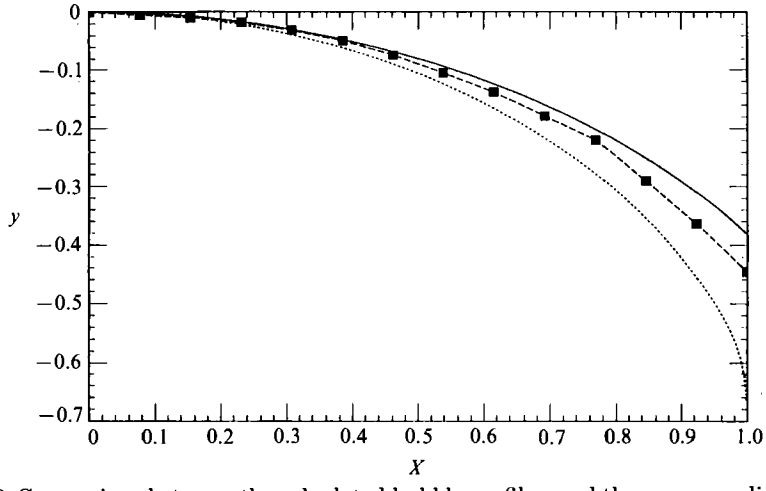

FIGURE 8. Comparison between the calculated bubble profiles, and the corresponding experimental one (figure 5*b* in Wegener & Parlange 1973) for the three-dimensional spherical cap bubble. Notation on figure 7.

region). This is apparent in figures 7 and 8 where we compare the calculated bubble profiles with the corresponding experimental ones. The agreement is excellent in the tip region, whereas there are deviations further downstream where the influence of the wake becomes stronger.

5. Discussion

We now wish to discuss, in retrospect, our idea that the surface tension controls the rise velocity through its effect on the tip of the bubble. This was initially an assumption which motivated this approach, but now can be considered justified given the comparison in §4 between the experimental data and the results from the

two different theoretical models. We must make use of this assumption to disregard the discrepancy in the equation at the bubble–wake connection point when the surface tension is non-zero. We now outline exactly why the discrepancy appears.

Let us first discuss the stagnant wake model. Here, the bottom shape of a spherical cap bubble plays no role in determining its top shape, as it does not enter the equations describing the top part. The shape of the bottom part of the bubble is balanced by the surface tension and the hydrostatic pressure drop, see Vanden-Broeck (1986). The equation describing the bottom shape is just a second order ordinary differential equation, with two boundary conditions: (*a*) the tangent is zero at $x = 0$; (*b*) it connects with the upper part at $x = 1$. In the absence of surface tension, the bottom shape is just a straight line (plane). In general the derivatives for the top and bottom shapes are discontinuous at the connection point $x = 1$ (see figure 1). The presence of a cusp when the surface tension is non-zero is certainly unphysical.

The singularity was by no means obvious when we started solving the exterior problem (determining the top bubble profile and wake shape), because the bottom shape of the bubble did not enter the equations of the exterior problem. It turned out that we failed to find a solution when a small surface tension was added to the problem, whereas the same program converged quickly to a solution at zero surface tension. This implies a presence of a singularity when the surface tension is non-zero, even though this is not apparent from the equations (13) and (22).

For the vertical wake model, the reason for the model breaking down when the surface tension is non-zero is more obvious. It is because the curvature at the connection point is infinite for all the zero-surface-tension solutions. We have numerical evidence to support this idea, but the easiest way to see it is to calculate the curvature for the Zhukovskii solution (3). Because of this, one is bound to have trouble near the connection point when the surface tension is non-zero.

Hence, both models break down around the connection point when the surface tension is non-zero. Thus strictly speaking, one can no longer use them for such a case, since they are not mathematically consistent. In order to have a completely consistent theory which is valid under finite surface tension, new models must be used. However, since we are only interested in cases where surface tension is very small, we argue that we can make a simple modification to our original models to incorporate the surface tension effect: the method we used was to not enforce the set of integro-differential equations near the connection point. As we will discuss below, the final results are insensitive to what precise approximations one uses near the connection point.

Vanden-Broeck (1986, 1988) has done calculations for both models of the two-dimensional spherical cap bubble problem using entirely different numerical methods. We have already compared our numerical results with his in the previous section. Here we take a look at the way he dealt with the singularities of the two models when the surface tension is non-zero.

For the two-dimensional stagnant wake model, no additional measure was taken in the program when the surface tension became non-zero. As a result the method broke down when the surface tension was small. To be more precise, the primary branch of the solution ended before the surface tension reached zero. One should not expect this from the continuity property of the problem. This failure could be attributed to the fact that the presence of the additional singularity when the surface tension became non-zero was not captured in the original power series expansion of the zero surface tension solutions.

For the two-dimensional vertical wake model, a tangential discontinuity was introduced at the connection point when the surface tension became non-zero. One can easily show via a local analysis of the Laplace equation that the velocity at the connection point will be infinite in this case. Provided the proper limit is taken, it is then possible to balance the velocity-squared and the curvature terms in Bernoulli's law. Vanden-Broeck was able to show numerically that the problem was well defined after introducing this discontinuity. We also tried this tangential discontinuity approach in our numerical method; it did not work well. This is probably because Vanden-Broeck's numerical method used the derivative of Bernoulli's law, whereas we used Bernoulli's law directly. In other words, the presence of two infinite terms in the equation could be factored out after taking the derivative. We eventually used a different approximation at the connection point when the surface tension was non-zero. Our approximation was from numerical point of view, namely we did not enforce the integro-differential equations rigorously near the connection point. Despite using a completely different numerical method and a completely different approximation at the connection point, our conclusions are the same as his. This clearly supports the idea that the bubble rise velocity is determined by the tip region, and it is insensitive to the approximation at the connection point.

The breakdown of these two models becomes more evident as the surface tension increases. The numerical evidence for this is that we can no longer find solutions using the modified method when γ becomes large. Besides the reasons mentioned above, there is an additional physical reason behind this breakdown. In such situations, the bubble will probably cease to be spherical cap and will become ellipsoidal or spherical, see Haberman & Morton (1956), which cannot be studied by simple extension of the two models used here.

We wish to thank J. Greene and C. Pozrikidis for some helpful suggestions.

REFERENCES

Collins, R. 1965 A simple model of the plane gas bubble in a finite liquid. *J. Fluid Mech.* **22**, 763–771.

Collins, R. 1967*a* The effect of a containing cylindrical boundary on the velocity of a large gas bubble in a liquid. *J. Fluid Mech.* **28**, 97–112.

Collins, R. 1967*b* The cycloidal bubble: A neglected solution in the theory of large plane gas bubbles in liquids. *Chem. Engng Sci.* **22**, 89–97.

Couët, B. & Strumolo, G. S. 1987 The effects of surface tension and tube inclination on a two-dimensional rising bubble. *J. Fluid Mech.* **184**, 1–14.

Davies, R. M. & Taylor, G. I. 1950 The mechanics of large bubbles rising through extended liquids and through liquids in tubes. *Proc. R. Soc. Lond.* A **200**, 375–390.

Grace, J. R. & Harrison, D. 1967 The influence of bubble shape on the rising velocities of large bubbles. *Chem. Engng Sci.* **22**, 1337–1347.

Gurevich, M. I. 1965 *Theory of Jets in Ideal Fluids.* Academic.

Haberman, W. L. & Morton, R. K. 1956 An experimental study of bubbles moving in liquids. *Trans. ASCE* **121**, 227–252.

Hnat, J. G. & Buckmaster, J. D. 1976 Spherical cap bubbles and skirt formation. *Phys. Fluids* **19**, 182–194.

Kessler, D. A. & Levine, H. 1989*a* Velocity selection for Taylor bubbles. *Phys. Rev.* A **39**, 5462–5465.

Kessler, D. A. & Levine, H. 1989*b* Steady-state cellular growth during directional solidification. *Phys. Rev.* A **39**, 3041–3052.

Lamb, H. 1932 *Hydrodynamics.* Dover.

LEVINE, H. & YANG, Y. 1990 A rising bubble in a tube. *Phys. Fluids* A **2**, 542–546.

LEVINSON, N. 1946 On the asymptotic shape of the cavity behind an axially symmetric nose moving through an ideal fluid. *Annals Maths* **47**, 704–730.

MANERI, C. C. & ZUBER, N. 1974 An experimental study of plane bubbles rising at inclination. *Intl J. Multiphase Flow* **1**, 623–644.

MAXWORTHY, T. 1967 A note on the existence of wakes behind large rising bubbles. *J. Fluid Mech.* **27**, 367–368.

RIPPIN, D. W. T. & DAVIDSON, J. F. 1967 Free streamline theory for a large gas bubble in a liquid. *Chem. Engng Sci.* **22**, 217–228.

VANDEN-BROECK, J. M. 1984*a* Bubbles rising in a tube and jets falling from a nozzle. *Phys. Fluids* **27**, 1090–1093.

VANDEN-BROECK, J. M. 1984*b* Rising bubbles in a two-dimensional tube with surface tension. *Phys. Fluids* **27**, 2604–2607.

VANDEN-BROECK, J. M. 1986 Free streamline model for a rising bubble. *Phys. Fluids* **29**, 2798–2801.

VANDEN-BROECK, J. M. 1988 Joukovskii's model for a rising bubble. *Phys. Fluids* **31**, 974–977.

VAN DYKE, M. D. 1982 *An Album of Fluid Motion.* Parabolic.

WEGENER, P. & PARLANGE, Y. 1973 Spherical-cap bubbles. *Ann. Rev. Fluid Mech.* **5**, 79–100.